

Additional file 2: Supplementary figures

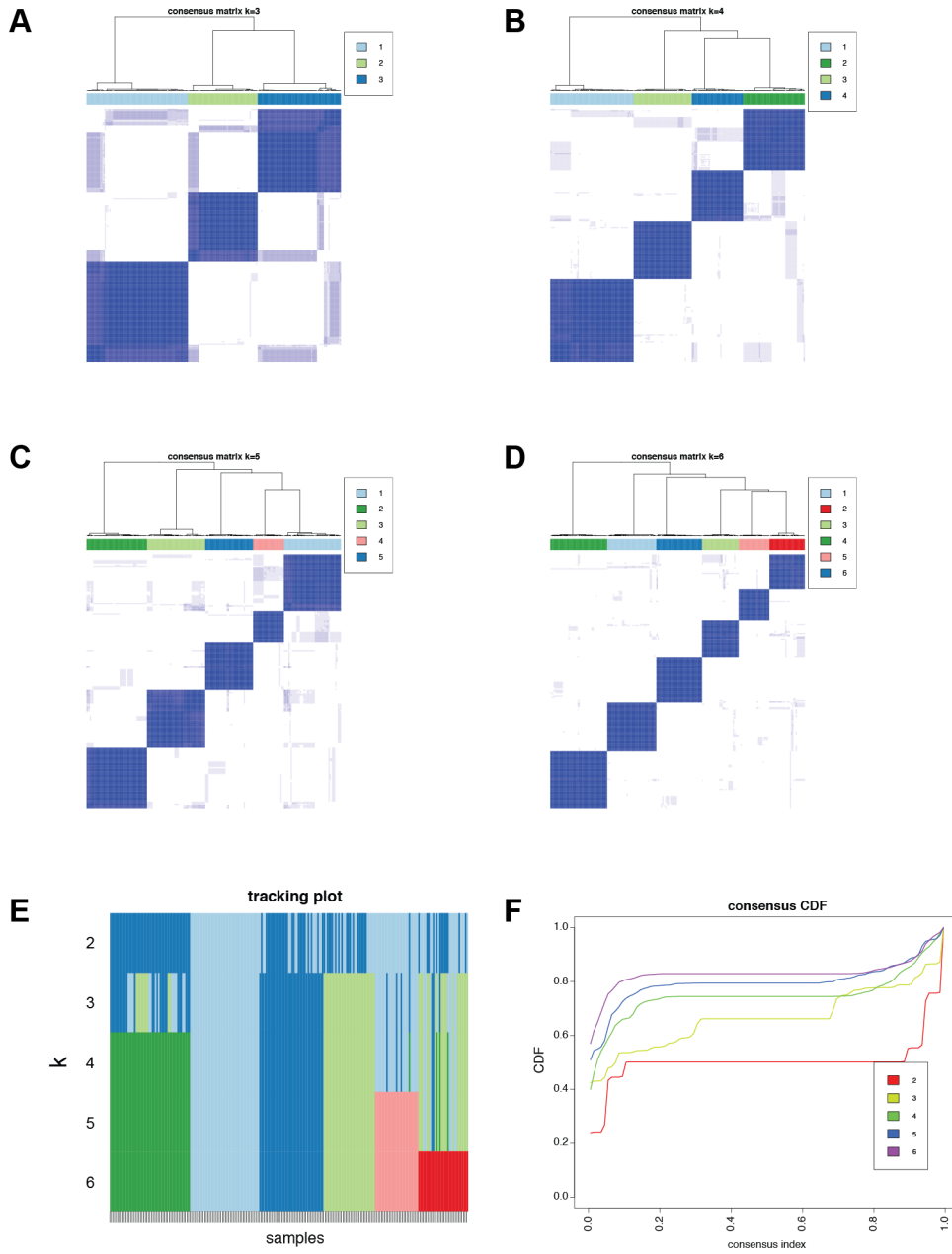


Figure S1: Consensus cluster plus output from unsupervised clustering of 750 highly variant lncRNAs in the NAC cohort. (A-D) Consensus membership heatmaps for the (A) 3-cluster solution, (B) 4-cluster solution, (C) 5-cluster solution, (D) 6-cluster solution, (E) tracking plot, and (F) Cumulative Distribution Function (CDF) plot of consensus membership values for solutions with between 2 and 6 clusters.

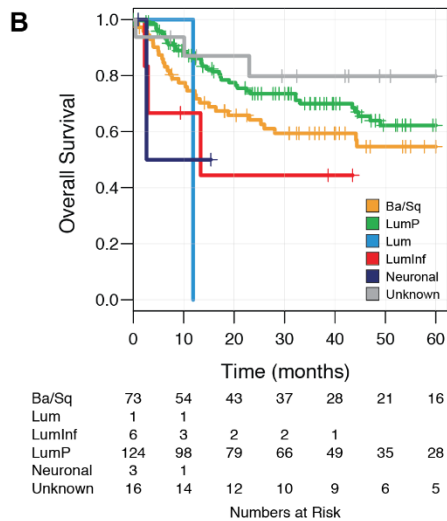
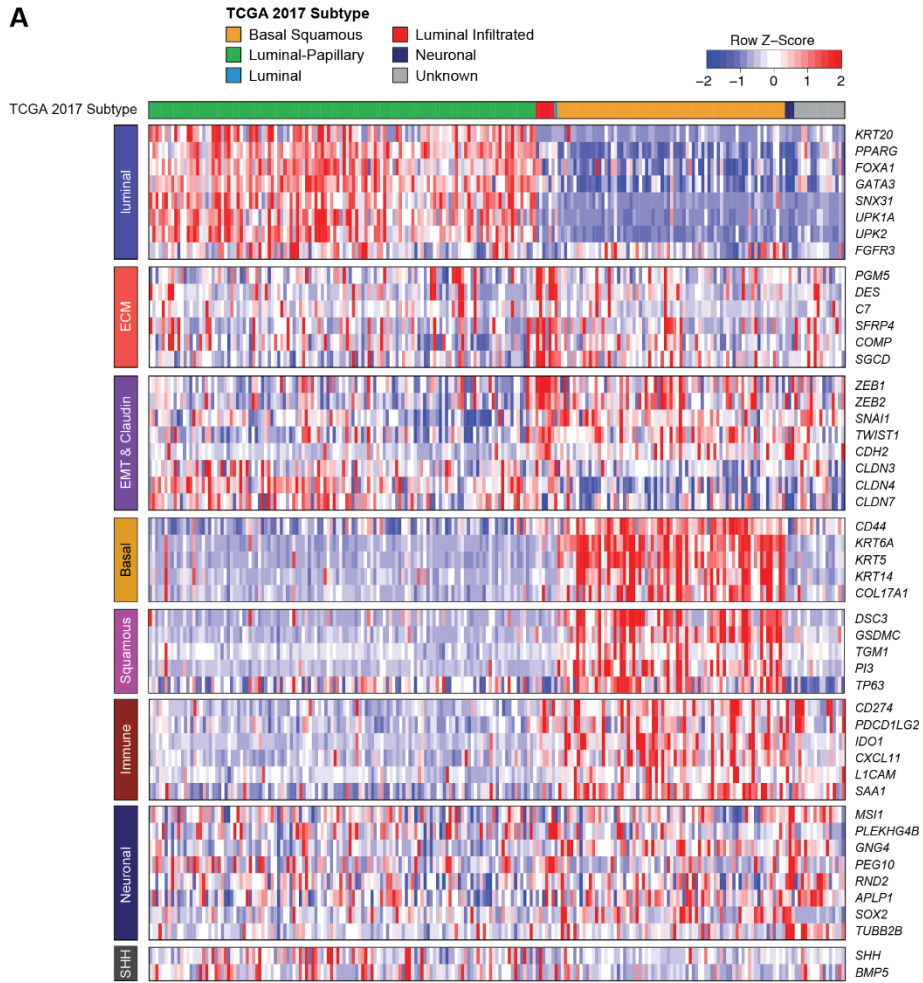
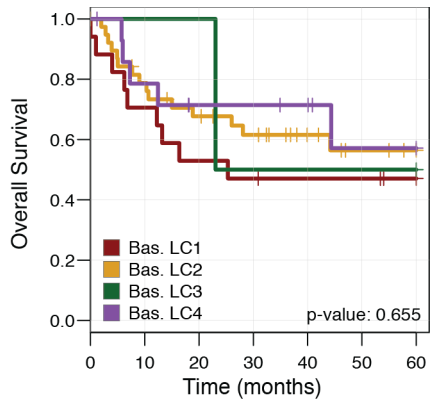


Figure S2: Molecular subtyping of the NAC cohort using the TCGA 2017 classifier. (A) Heatmap of the five TCGA subtypes (luminal-papillary, luminal, luminal infiltrated, basal squamous and neuronal) and unknown. (B) KM plot of the NAC cohort stratified by the TCGA 2017 classifier.



| | | | | | | | |
|----------|----|----|----|----|----|---|---|
| Bas. LC1 | 17 | 12 | 9 | 8 | 7 | 7 | 4 |
| Bas. LC2 | 39 | 29 | 24 | 20 | 13 | 9 | 7 |
| Bas. LC3 | 2 | 2 | 2 | 1 | 1 | 1 | 1 |
| Bas. LC4 | 15 | 11 | 5 | 8 | 7 | 4 | 4 |

Numbers at Risk

Figure S3: Survival analysis for IncRNA clusters stratified by the basal/squamous mRNA subtype in the NAC cohort.

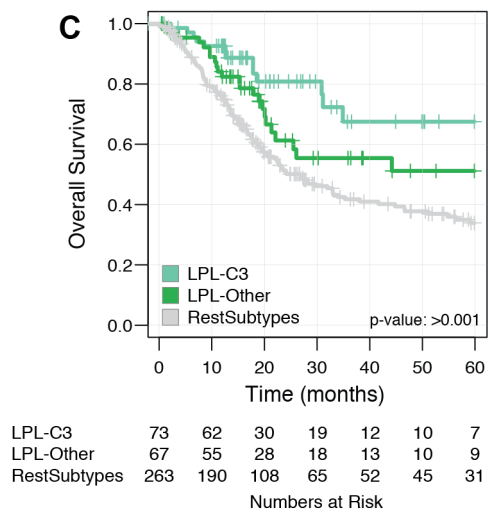
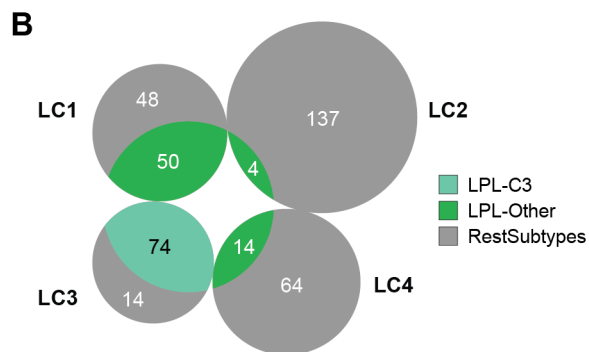
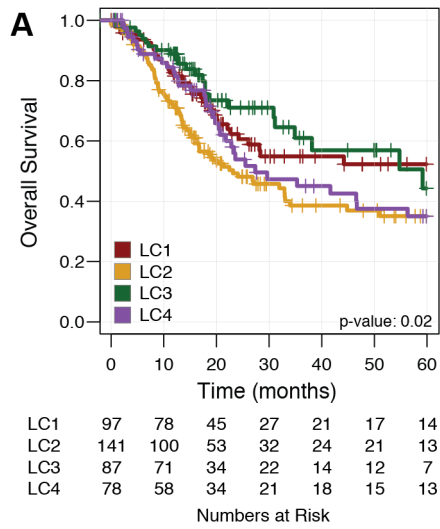


Figure S4. Survival analysis for IncRNA clusters in TCGA cohort. (A) KM plot for IncRNA clusters (LC1-4) in the TCGA cohort, (B) Intersection of the IncRNA clusters (LC1-4) with the luminal papillary mRNA subtype and (C) KM plot for IncRNA-split luminal papillary tumors (LPL-C3, LPL-Other).

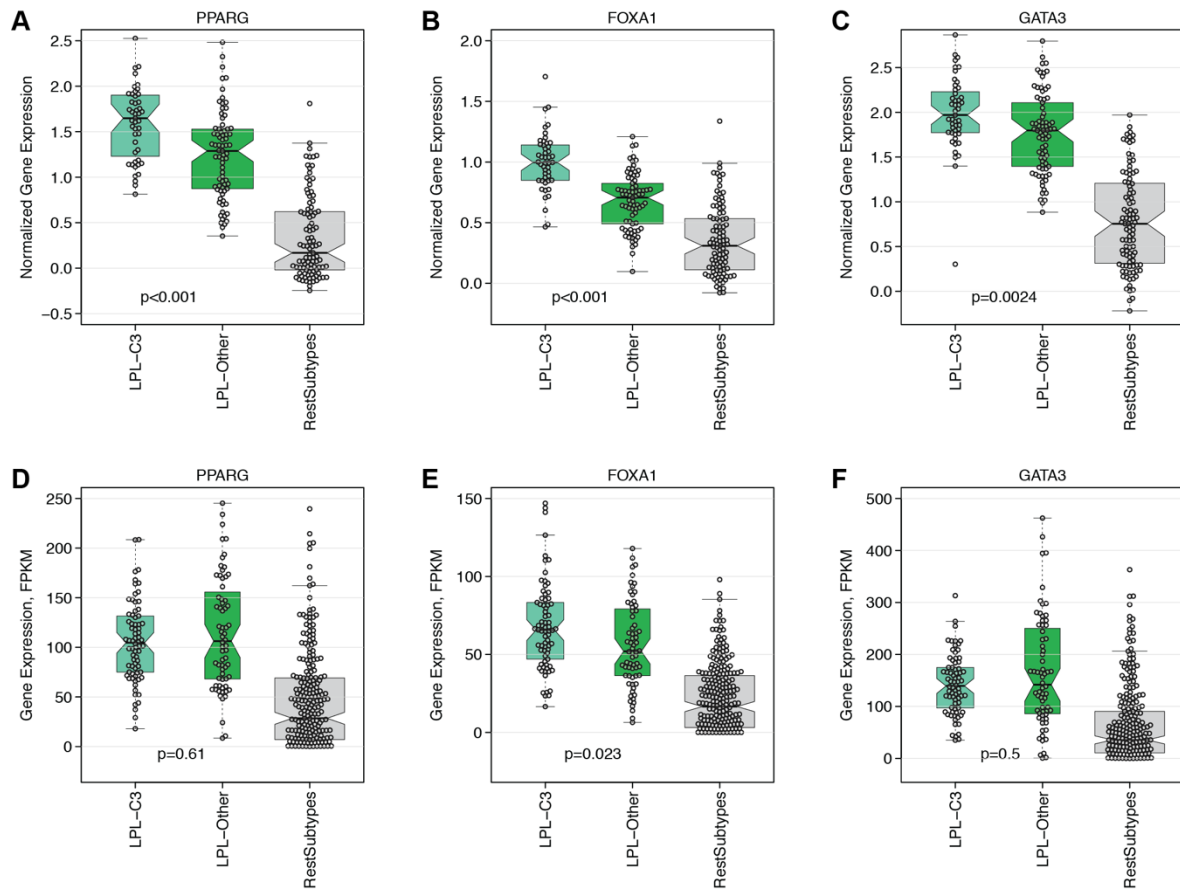


Figure S5: Expression of select MIBC marker genes associated with the luminal subtype in the LPL-C3 and LPL-Other tumors, for the NAC cohort (A) *PPARG*, (B) *FOXA1*, (C) *GATA3* and TCGA cohort (D) *PPARG*, (E) *FOXA1*, (F) *GATA3*, respectively.

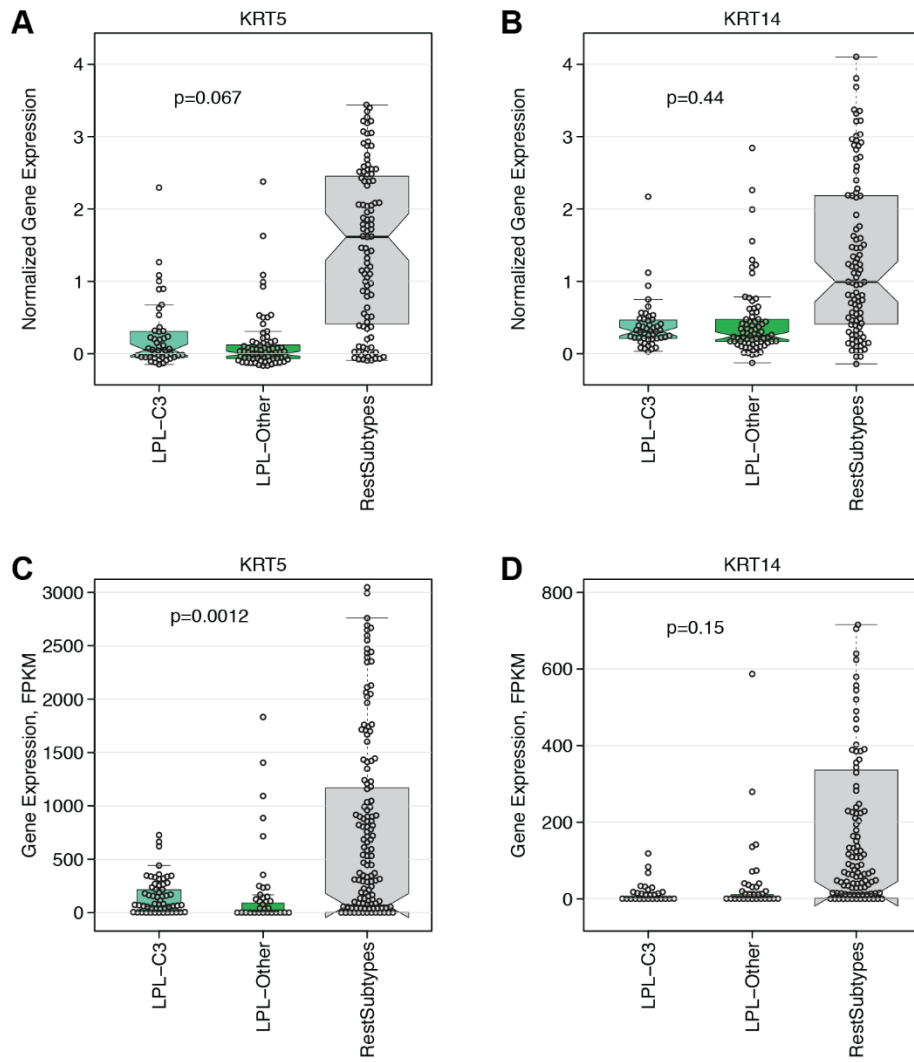


Figure S6: Expression of select MIBC marker genes associated with the basal subtype in the LPL-C3 and LPL-Other tumors, for the NAC cohort (A) *KRT5*, (B) *KRT14* and TCGA cohort (C) *KRT5*, (D) *KRT14*, respectively.

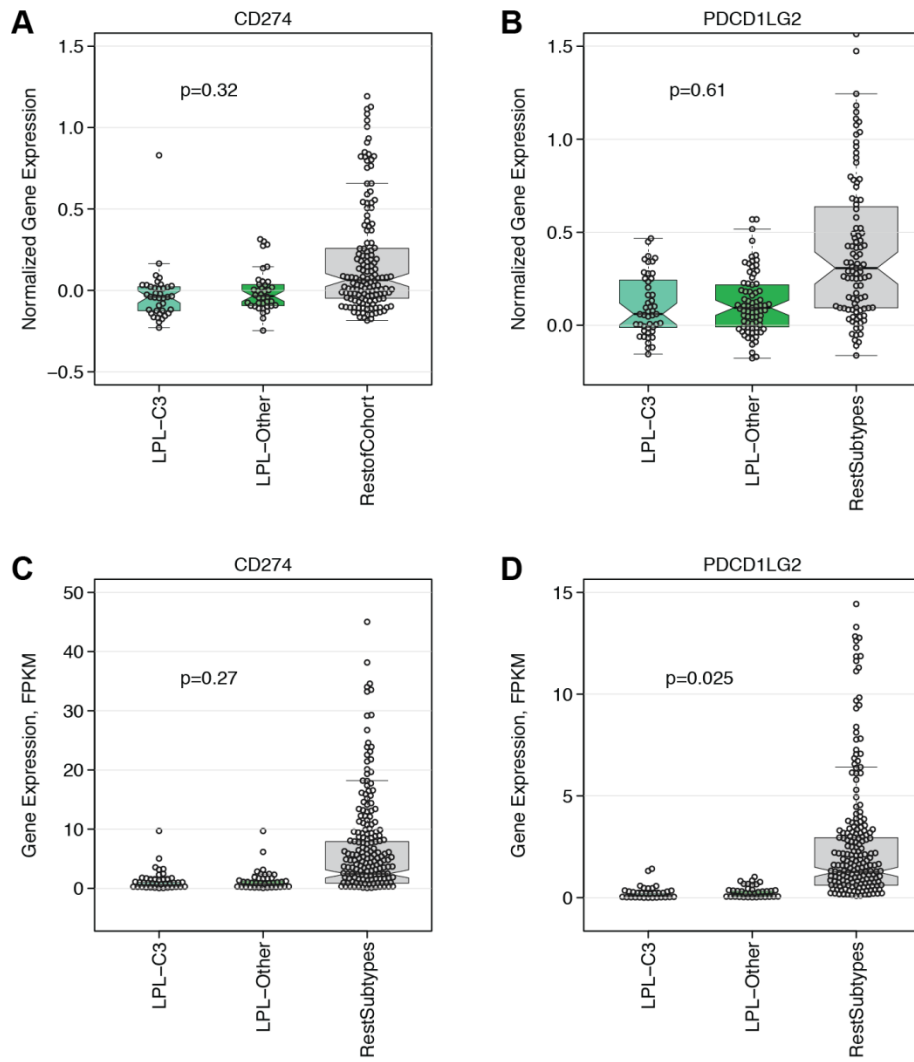


Figure S7: Expression of select MIBC marker genes associated with the immune oncology in the LPL-C3 and LPL-Other tumors, for the NAC cohort (A) *CD274* (PD-L1), (B) *PDCD1LG2* (PD-1) and TCGA cohort (C) *CD274* (PD-L1), (D) *PDCD1LG2* (PD-1), respectively.

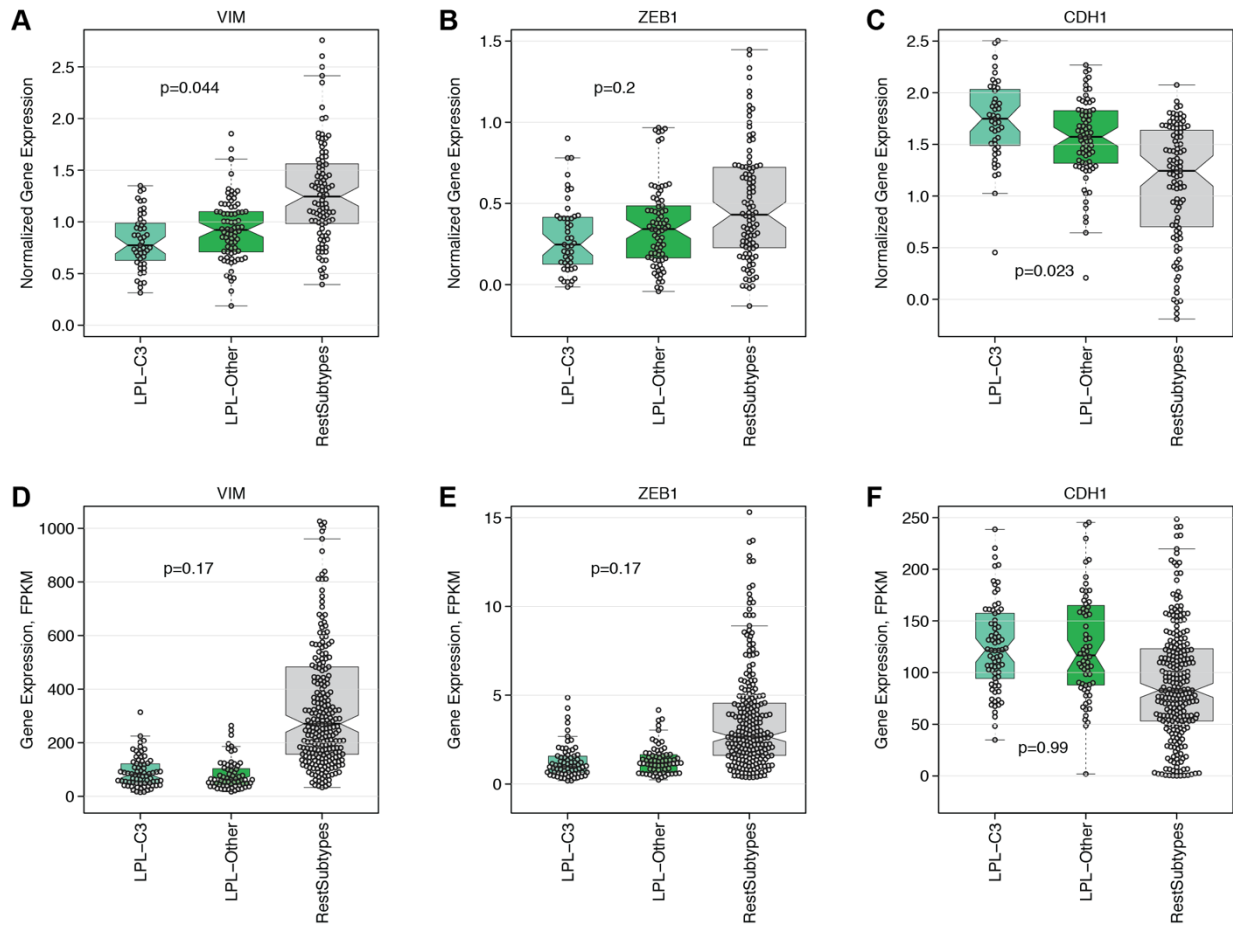


Figure S8: Expression of select genes associated with EMT in the LPL-C3 and LPL-Other tumors, for the NAC cohort (A) *VIM*, (B) *ZEB1*, (C) *CDH1* and TCGA cohort (D) *VIM*, (E) *ZEB1*, (F) *CDH1*, respectively.

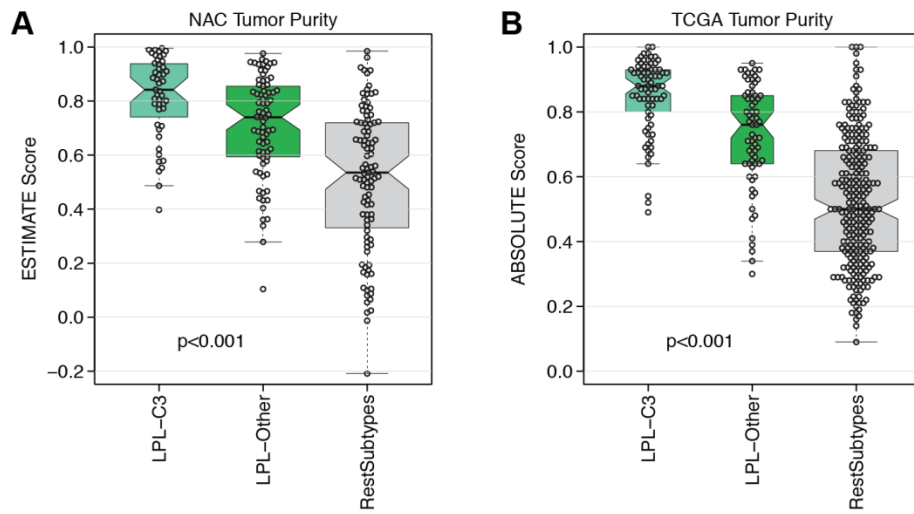


Figure S9: Sample purity estimates for the (A) NAC cohort using the ESTIMATE algorithm and (B) TCGA using the ABSOLUTE algorithm (previously calculated).

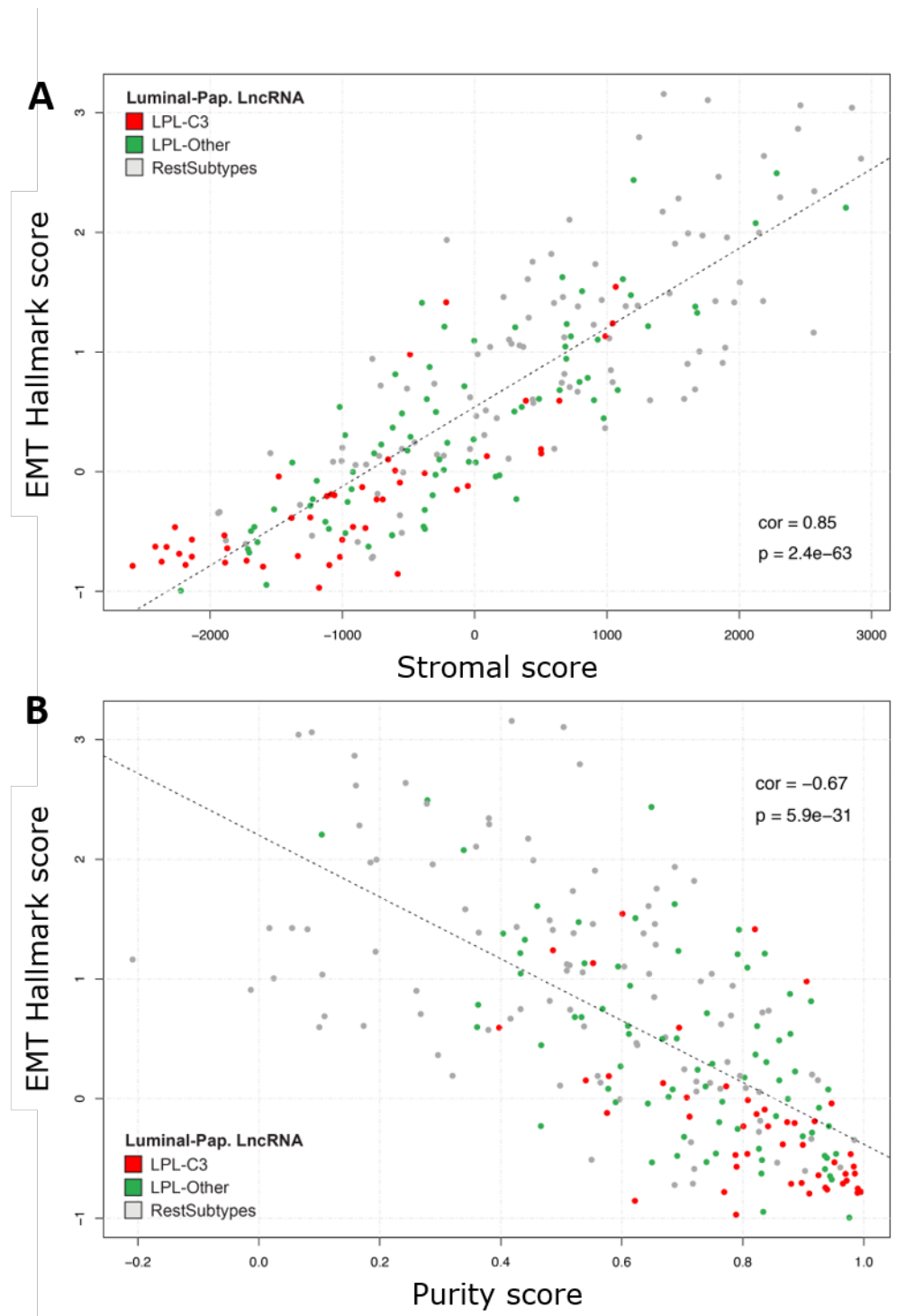


Figure S10: Scatterplots for the observed correlation between EMT hallmark scores and (A) stromal and (B) purity estimates, using the NAC cohort and the ESTIMATE algorithm.

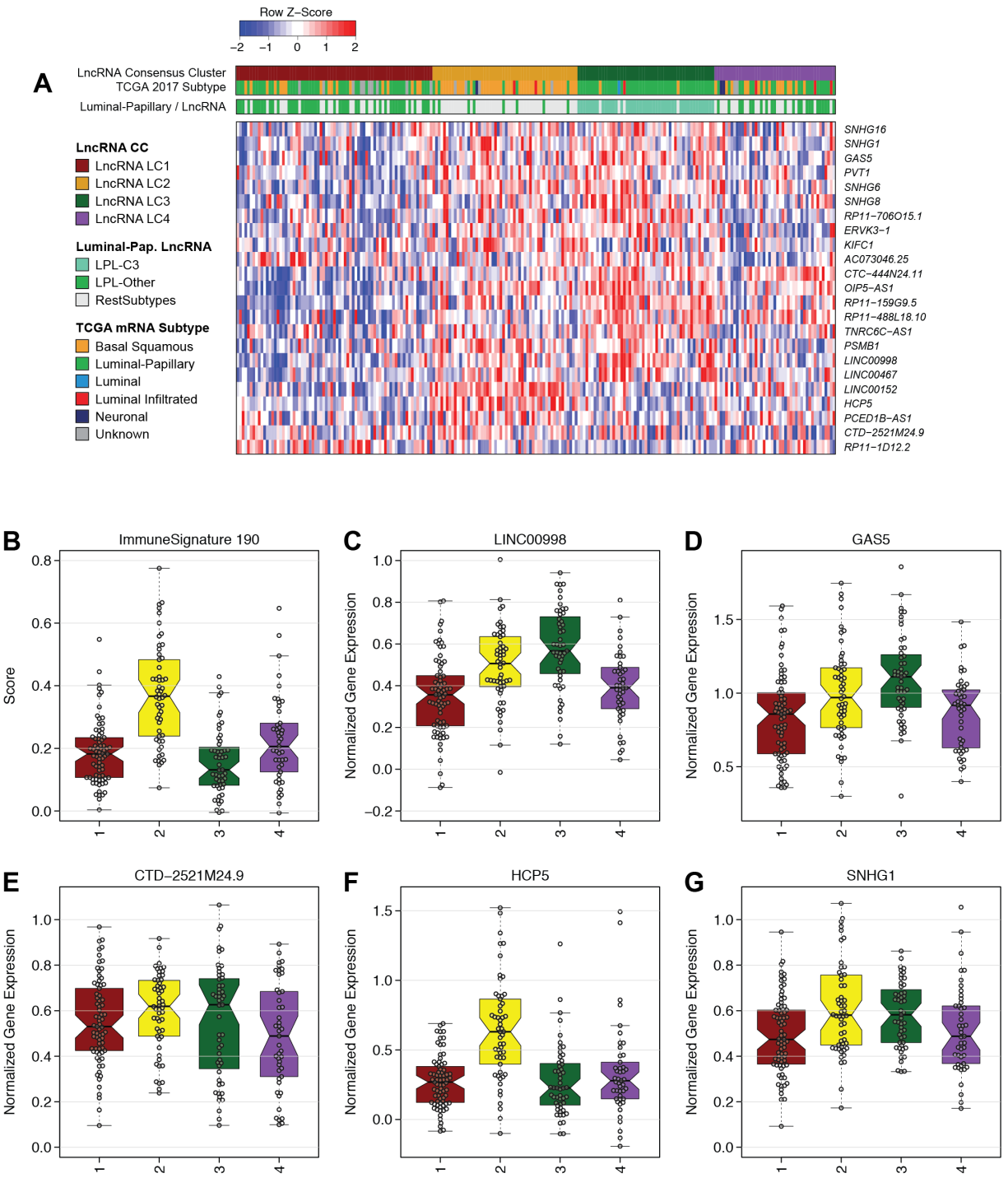


Figure S11: Contribution of immune-associated lncRNAs to consensus clustering solution in the NAC cohort. (A) Heatmap of 23 lncRNAs highly expressed in lymphocytes and contributing to lncRNA-clustering. (B) Immune190 signature score indicating immune-infiltration levels. LncRNA expression levels for (C) *LINC00998*, (D) *GAS5*, (E) *CTD-2521M24.9*, (F) *HCP5* and (G) *SNHG1*.

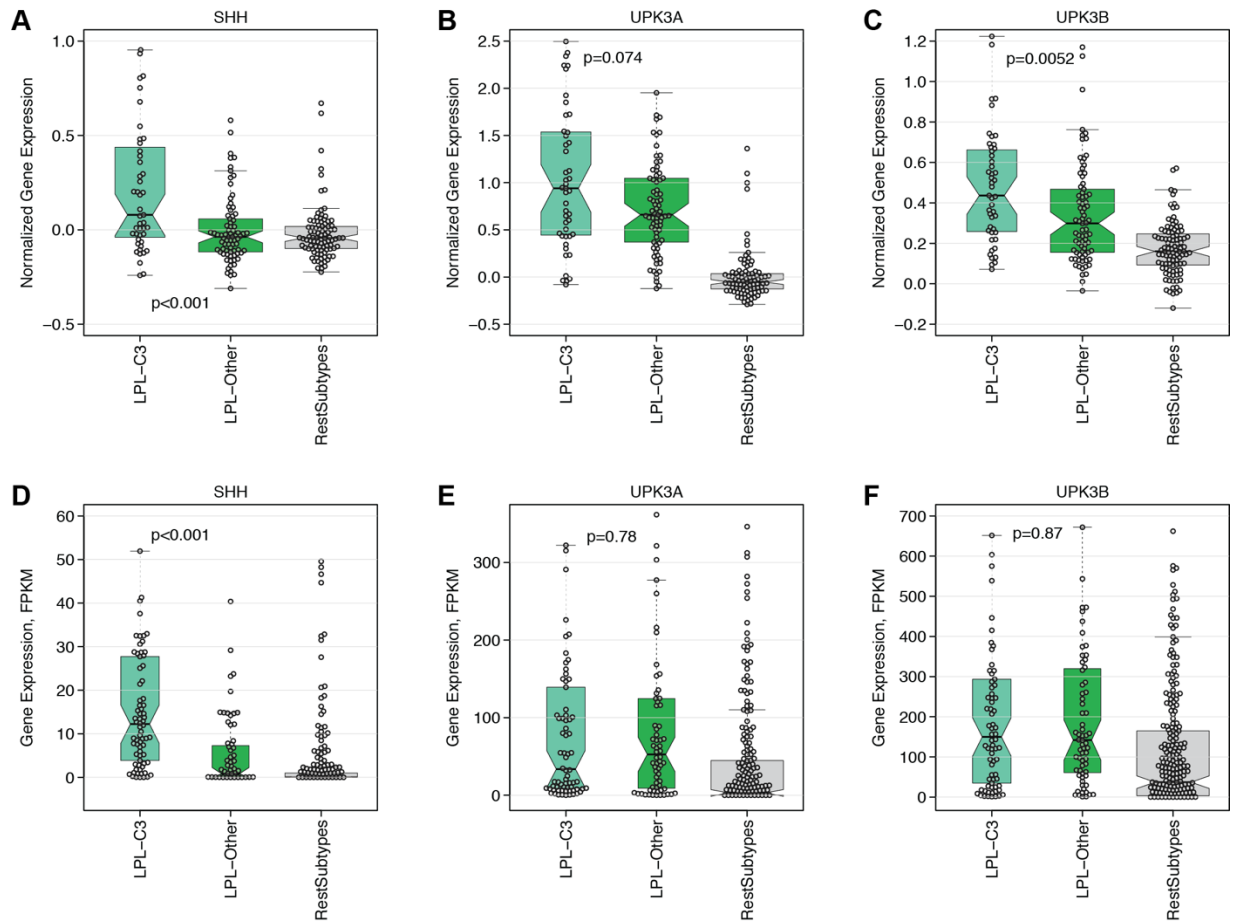


Figure S12: Expression of select genes associated with SHH and urothelial differentiation in the LPL-C3 and LPL-Other tumors, for the NAC cohort (A) *SHH*, (B) *UPK3A*, (C) *UPK3B* and TCGA cohort (D) *SHH*, (E) *UPK3A*, (F) *UPK3B*, respectively.

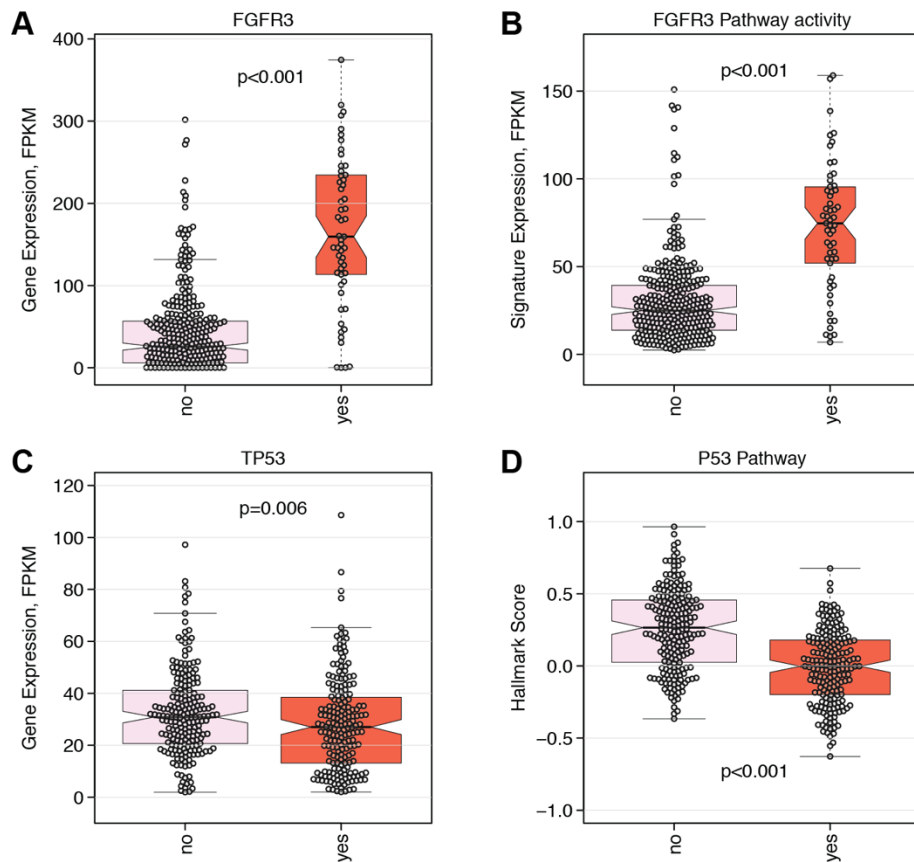


Figure S13: Correlation of gene expression and pathway activity with respect to mutation status in the TCGA cohort. (A) *FGFR3* gene expression, (B) *FGFR3* pathway activity, (C) *TP53* gene expression and (D) p53 pathway activity. For each panel, 'no' indicates wild-type and 'yes' indicates a mutation.

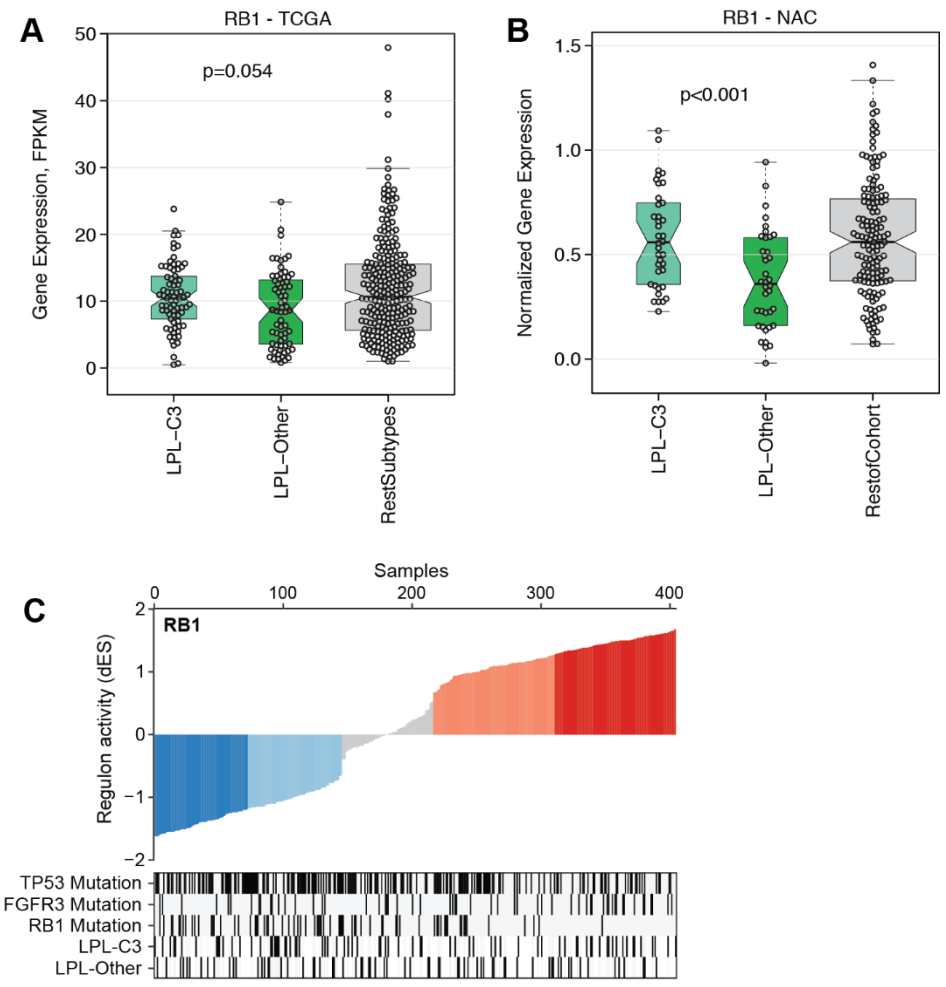


Figure S14: RB1 expression in (A) TCGA and (B) NAC cohorts. (C) RB1 regulon activity scores in TCGA cohort with *TP53*, *FGFR3* and *RB1* mutation status and LPL-C3 vs. LPL-Other indicated in covariate tracks. A dark black bar indicates a mutation event.

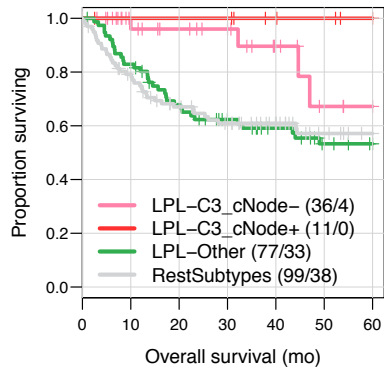


Figure S15: Survival analysis of LPL-C3 patients with (LPL-C3 cNode+) and without (LPL-C3 cNode-) clinically node positive disease.

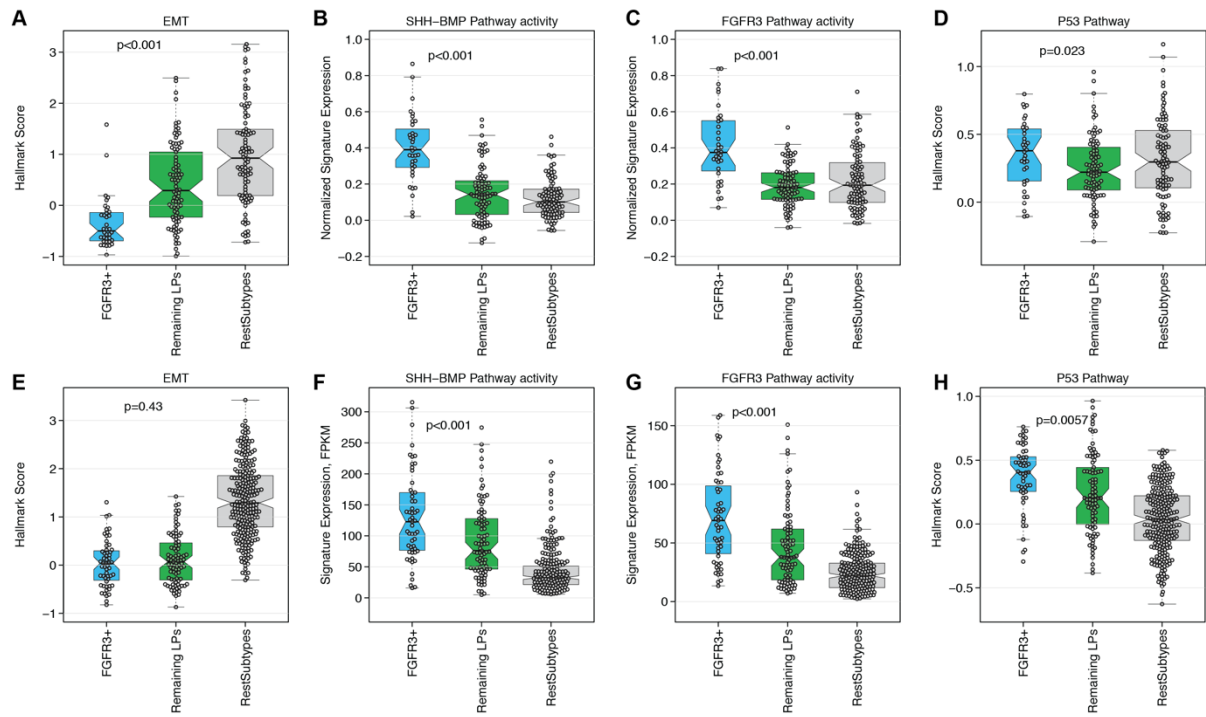


Figure S16: Biological pathways differentially activated between tumors classified as FGFR3+ by the GC and other tumors. For the NAC cohort (A) EMT hallmark activity, (B) SHH-BMP pathway activity, (C) FGFR3 signature score, (D) p53 hallmark activity. The TCGA cohort follows the same order for panels E-H.

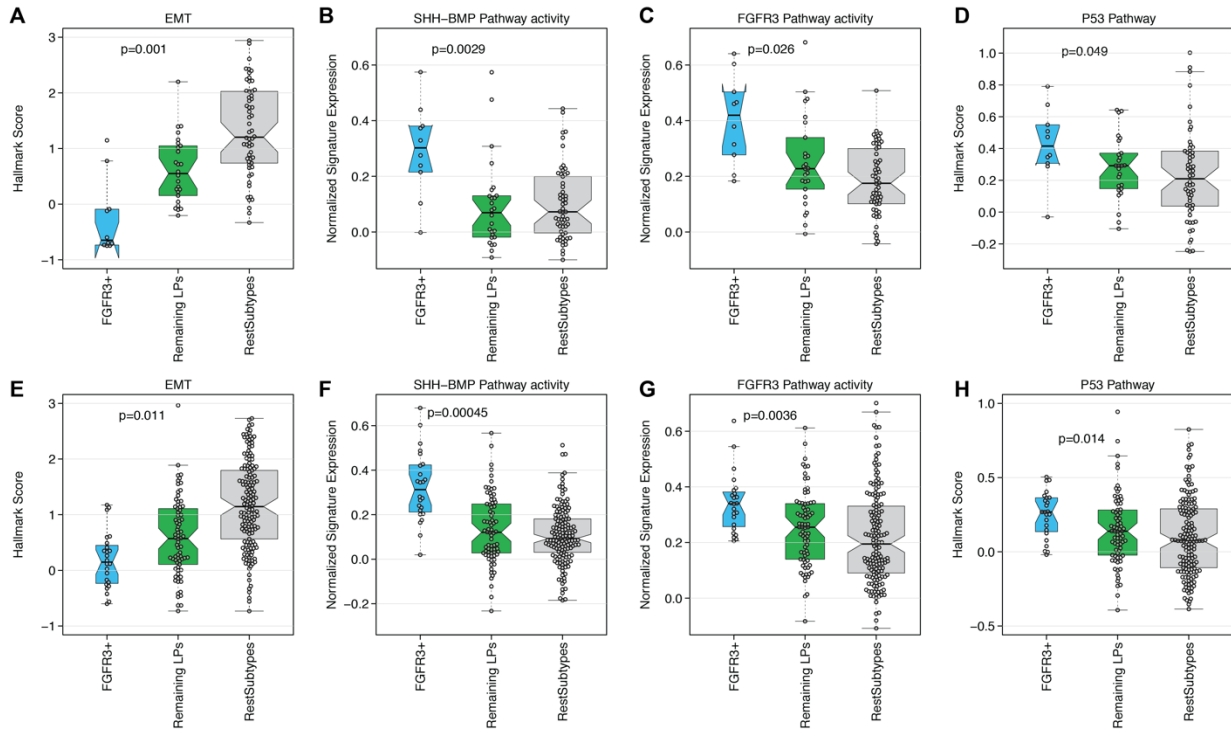


Figure S17: Biological pathways differentially active between tumors classified as FGFR3+ by the GC and other tumors. For the UTSW cohort (A) EMT hallmark activity, (B) SHH-BMP pathway activity, (C) FGFR3 signature score, (D) p53 hallmark activity. The PCC cohort follows the same order for panels E-H.